RESEARCH ARTICLE

National Science Open
2: 20230033, 2023
https://doi.org/10.1360/nso/20230033

Materials Science

A new artificial photosynthetic system coupling photovoltaic electrocatalysis with solar heating catalysis

Yaguang Li[1,#,*], Fanqi Meng[2,#], Xianhua Bai[1,#], Dachao Yuan[3], Xingyuan San[1], Shufang Wang[1], Lin Gu[2] & Qingbo Meng[2,*]

[1]*Research Center for Solar Driven Carbon Neutrality, Hebei Key Lab of Optic-electronic Information and Materials, The College of Physics Science and Technology, Institute of Life Science and Green Development, Hebei University, Baoding 071002, China;*
[2]*Beijing National Laboratory for Condensed Matter Physics, Institute of Physics, Chinese Academy of Sciences, Beijing 100190, China;*
[3]*College of Mechanical and Electrical Engineering, Hebei Agricultural University, Baoding 071001, China*

#Contributed equally to this work.
*Corresponding authors (emails: liyaguang@hbu.edu.cn (Yaguang Li); qbmeng@iphy.ac.cn (Qingbo Meng))

Received 12 June 2023; Revised 28 June 2023; Accepted 10 July 2023; Published online 22 August 2023

Abstract: In this work, we present a novel artificial photosynthetic paradigm with square meter (m^2) level scalable production by integrating photovoltaic electrolytic water splitting device and solar heating CO_2 hydrogenation device, successfully achieving the synergy of 1 sun driven 19.4% solar to chemical energy efficiency (STC) for CO production (2.7 times higher than that of large-sized artificial photosynthetic systems) with a low cost (equivalent to 1/7 of reported artificial photosynthetic systems). Furthermore, the outdoor artificial photosynthetic demonstration with 1.268 m^2 of scale exhibits the CO generation amount of 258.4 L per day, the STC of ~15.5% for CO production in winter, which could recover the cost within 833 sunny days of operation by selling CO.

Keywords: artificial photosynthetic, photovoltaic electrocatalysis, solar heating catalysis, CO_2 hydrogenation, low cost

INTRODUCTION

Artificial photosynthesis can convert CO_2 and H_2O into useful fuels, chemicals (CO [1], CH_4 [2], etc.) and O_2 under solar irradiation, which is the most important way for carbon neutralization [3–9]. The application of large-scale artificial photosynthesis is of great significance to weaken the global warming, overcome the current energy and environmental crisis [10–12]. More recently, several large-sized artificial photosynthetic systems for CO_2 utilization have been reported, e.g., the solar fuel production chain with square meters (m^2) scale [13], the photovoltaic electrocatalytic device with ~0.1 m^2 scale [14]. To the best of our knowledge, the highest solar to chemical energy efficiency (STC) of large-sized devices is 7.2% by the photovoltaic electrocatalytic system [14]. However, the material cost for constructing large-sized artificial photosynthetic system is too expensive to practical application, due to the using of noble metal catalysts (e.g., Ir, Pt, Rh, Ru) and the costliness of large-sized components (e.g., membranes, solar reactor) in the devices [15,16]. Therefore, it is one of the holy grails of the entire scientific and technological community to achieve a scalable artificial photosynthetic system with high STC and low cost simultaneously, so as to realize the

sustainable development of human society.

Herein, we have developed a new artificial photosynthetic system by integrating a photovoltaic electrolytic H_2O decomposition part and a solar heating CO_2 hydrogenation part. Just relying on such a simple strategy, this system not only changed the reaction path and mass transportation but also discarded all rare elements and expensive components, resulting in the m^2 level scalable production and a record STC (19.4%) with low cost. Moreover, an outdoor demonstration (1.268 m^2 scale) of this new design was built based on full commercial components and the STC was still higher than 15% at outdoor test in winter. This artificial photosynthetic system could recover the total system cost within 833 days of operation by selling the products of CO.

METHOD SECTION

Thermocatalytic CO_2 hydrogenation

The thermocatalytic activity of catalysts for CO_2 hydrogenation was tested by the fixed-bed reactor (XM190708-007, Dalian Zhongjiaruilin Liquid Technology Co., Ltd.) in continuous flow form. Typically, 10 mg of catalyst was placed in a quartz flow reactor. For CO production, the feed gas of $CO_2/H_2/Ar$ = 1:1:48 or CO_2/99% H_2+1% O_2/Ar = 1:1:48 with 100 sccm of flow rate was regulated by the mass flow controller. The reaction products were tested by gas chromatograph (GC) 7890A equipped with FID and TCD detectors.

Solar heating CO_2 hydrogenation as CO

The solar heating CO_2 hydrogenation was tested as follows. 137 g of Fe SACs were loaded intoTiC/Cu based device (0.024 m^2), and irradiated by a xenon lamp (ZSL-4000). In this test, CO_2 and 100% H_2 (or 99% H_2 +1% O_2) were mixed as feed gas. For the produced gas, the flow rate was tested by mass flowmeter and the composition was tested by GC 7890A equipped with FID and TCD detectors. The data were collected by FID and TCD.

The CO rate (δ, mol m^{-2} h^{-1}) was calculated as follows:

$$\delta(\text{mol m}^{-2}\text{h}^{-1}) = L / (24.5 \times S) \quad (1)$$

where L is the CO flow rate (L h^{-1}), S is the irradiated area (0.024 m^{-2}). When using the 99% H_2+1% O_2 as feed gases, the L irradiated by 0.6, 0.8, and 1 sun was 0.98, 5.32, and 12.43 L h^{-1}, respectively.

Solar driven water splitting

The back contact silicon cells interdigitated with 2800 cm^2 irradiation area were purchased from SUN-POWER (23.5% efficiency) to drive an alkaline electrolyzer with 1 m^2 of Ni/Stainless steel mesh. Xenon lamp (HP-2-4000) was used as a light source and 1 mol L^{-1} KOH was used as the electrolyte for sunlight driven water splitting. The produced H_2 was injected into the TiC/Cu based device and the produced H_2 rate of the solar driven water splitting system was tested by mass flowmeter (C50 300SCCM).

The H_2 production rate for per m^2 (H, mol m^{-2} h^{-1}) of solar cell was calculated as follows:

$$H(\text{mol m}^{-2}\text{ h}^{-1}) = \varepsilon / (24.5 \times S) \quad (2)$$

where ε (L h^{-1}) is the H_2 generation amount per hour detected by a flowmeter, S is the irradiated area (0.2800 m^{-2}). The ε irradiated by 0.4, 0.6, 0.8, and 1 sun was 6.68, 10.02, 13.31, and 16.45 L h^{-1}, respectively.

Enthalpy change energy of chemicals

The enthalpy change energy of CO_2(g), CO(g), H_2(g), O_2(g), H_2O(g), and H_2O(l) was −393.505, −110.541, 0, 0, −241.818, and −285.830 kJ mol^{-1}, respectively.

The (g) and (l) indicated the gas state and liquid state, respectively.

Novel artificial photosynthesis for CO_2 and H_2O converted as CO and O_2

As the solar driven water splitting produced H_2 injected into the TiC/Cu based device loaded with 137 g of Fe SACs, CO_2 was simultaneously put into the TiC/Cu based device, which was controlled by mass flow controller (C50 5SLM). The TiC/Cu based device was irradiated by a xenon lamp (ZSL-4000). For the produced gas, the flow rate was tested by mass flowmeter (C50 5SLM) and the composition was tested by GC 7890A equipped with FID and TCD detectors.

The CO rate (δ, mmol h^{-1}) was calculated as follows:

$$\delta(\text{mmol h}^{-1}) = (1000 \times L / 24.5) \quad (3)$$

where L was the CO flow rate (L h^{-1}) and the L irradiated by 0.6, 0.8, and 1 sun was 0.946, 5.170, and 12.030 L h^{-1}, respectively.

The STC calculation of sunlight driven CO_2 conversion as CO

The STC efficiency of novel artificial photosynthetic system for converting CO_2 into CO was calculated as follows:

$$\text{STC} = (\Delta H \times \varepsilon) / (I \times S_T \times 3600) \quad (4)$$

where ΔH was the reaction enthalpy change energy (H_2O(l) + CO_2(g) → CO(g) + 1/2O_2(g) + H_2O(g), ΔH = 326.9754 kJ mol^{-1}), ε (mol) was the CO generation amount per hour detected by a flowmeter, I was the light intensity (kW m^{-2}), S_T was the total irradiated area. The ε irradiated by 0.6, 0.8, 1 sun was 0.0386, 0.211, 0.491 mol, respectively.

Since not all H_2 produced from solar driven water splitting was used for CO_2 hydrogenation, the irradiation area (β) of solar driven water splitting used for CO_2 hydrogenation was calculated as follows:

$$\beta = M / N \times 0.2800\ \text{m}^{-2} \quad (5)$$

The M was H_2 used for CO_2 hydrogenation as CO, which was equal to the CO production rates of 0.0386, 0.211, and 0.491 mol h^{-1}, under 0.6, 0.8, and 1 sun irradiation, respectively. The N was the H_2 production rate of 0.3931, 0.5273, and 0.6714 mol h^{-1}, irradiated by 0.6, 0.8, and 1 sun, respectively. Therefore, the β was 0.0276, 0.1119, and 0.2047 m^{-2}, under 0.6, 0.8, and 1 sun irradiation, respectively. And the

$$S_T = \beta + 0.0240\ \text{m}^{-2} \quad (6)$$

Therefore, the S_T was 0.0516, 0.1359, and 0.2287 m^{-2}, under 0.6, 0.8, and 1 sun irradiation, respectively.

Consequently, the STC was 11.3%, 17.6%, and 19.4%, under 0.6, 0.8, and 1 sun irradiation, respectively.

The EC calculation

The 1 sun driven EC of photovoltaic electrocatalytic water splitting in this work and reported photovoltaic electrocatalytic CO_2 reduction was calculated as follows:

$$EC = STCE / efficiency \quad (7)$$

The STCE was the solar to hydrogen chemical efficiency (19.04%) under 1 sun irradiation. The efficiency was the electric energy generation efficiency of solar cell (23.5%) under 1 sun irradiation. Therefore, the EC was calculated as 81.0%.

Outdoor artificial photosynthetic system

The outdoor artificial photosynthetic system consisted of two components. One component was photovoltaic electrolysis system, in which the PERC solar cell (182DCB) with 1.07 m^2 of solar irradiation area was used to power electrolytic reactor with 2.782 m^2 of Ni/Stainless steel mesh divided into 12 independent chambers in series. The mixture of 200 g KOH and 1.8 L deionized water was used as the electrolyte. The other component was solar heating system, in which a solar heating device was provided by Hebei scientist research experimental and equipment trade Co., Ltd. with the size of 4 cm in diameter and 50 cm inlength, eqquipped with a reflector of 50 cm inlength and 36 cm in width. For the production of CO, the catalysts used in solar heater were 400 g $CuO_x/ZnO/Al_2O_3$. For CO production production in solar heating system, the CO_2/H_2 ratio was > 1.5. It was required to control the flow rate to ensure the H_2 consumption. The data were collected by FID and TCD.

The STC of outdoor artificial photosynthetic system

The STC of the outdoor artificial photosynthetic system for converting CO_2 into CO was calculated as follows:

$$STC = (\Delta H \times \varepsilon) / (I \times S_T \times 3600 \times 22.4) \quad (8)$$

where ΔH is the reaction enthalpy change energy ($H_2O(l) + CO_2(g) \rightarrow CO(g) + 1/2O_2(g) + H_2O(g)$, ΔH = 326.9754 kJ mol^{-1}), ε (L) was the CO generation amount per hour detected by a flowmeter, I was the outdoor solar intensity (kW m^{-2}), S_T was the total irradiated area of 1.268 m^2.

The cost recovery calculation

We assumed that the CO production amount of the outdoor artificial photosynthetic system was 258.4 L day^{-1}. Due to the variety of CO prices, the quotation of Chae *et al*. [17] reported result and North Special Gas Co., Ltd. was adopted, which was \$6 per m^3 CO.

Therefore, the income of outdoor artificial photosynthetic system for CO production was 0.2584 × \$6 = \$1.55. To achieve an income of \$1291, this system required \$1291/\$1.55 = 833 sunny days, which were

equivalent to the sunny days in 3.5 years, according to the weather in Baoding of 240 sunny days per year.

RESULTS AND DISCUSSION

Conception for constructing novel artificial photosynthetic system

It is well known that the widely studied photovoltaic electrocatalytic systems contain the competition of two main reactions: H_2O decomposition and CO_2 hydrogenation on one system with CO_2 transportation through liquid electrolytes. Although various efficient catalysts have been developed, such as metals [18–20], metal compounds [21–23], molecular complexes [24,25], photovoltaic electrocatalysis still faces two intrinsic shortcomings: one is the complex reaction process in single catalytic site and the other is the sluggish CO_2 supply through gas/liquid transportation [26–28]. Here, a new paradigm of artificial photosynthesis is proposed to separate the two reactions of water splitting ($2H_2O \rightarrow 2H_2 + O_2$) [29] and CO_2 hydrogenation ($CO_2 + H_2 \rightarrow CO + H_2O$) [30–32] in space and time. There are four major advantages in this new system: (1) mature technologies can be selected for both water splitting and CO_2 hydrogenation; (2) the integrated system can be easy amplified; (3) the systems for the two reactions can be optimized separately, providing a variety of possibilities for efficiency, cost and products; (4) CO_2 supply can be boosted by avoiding the gas transport in liquid elelctrolytes. As shown in Figure 1, this is an integrated system in which the hydrogen generated from photovoltaic water electrolysis [33] is directly injected into the solar heating system for CO_2 hydrogenation [34–36]. The CO_2 transportation of this system is in gas diffusion mode at a rate of 10^{-5} m^2 s^{-1} [37], 10,000 times higher than the rate of CO_2 diffused through liquid electrolytes (10^{-9} m^2 s^{-1}) [38] in conventional photovoltaic electrocatalytic systems [39,40], which could meet the CO_2 supply for large-sized artificial photosynthetic systems. For integrating such a new artificial photosynthetic system, the two issues should be solved firstly. One is the matching problem of solar energy utilization in this system, that is, how to scientifically distribute the proportion of solar energy irradiated to the two devices to improve the STC; the

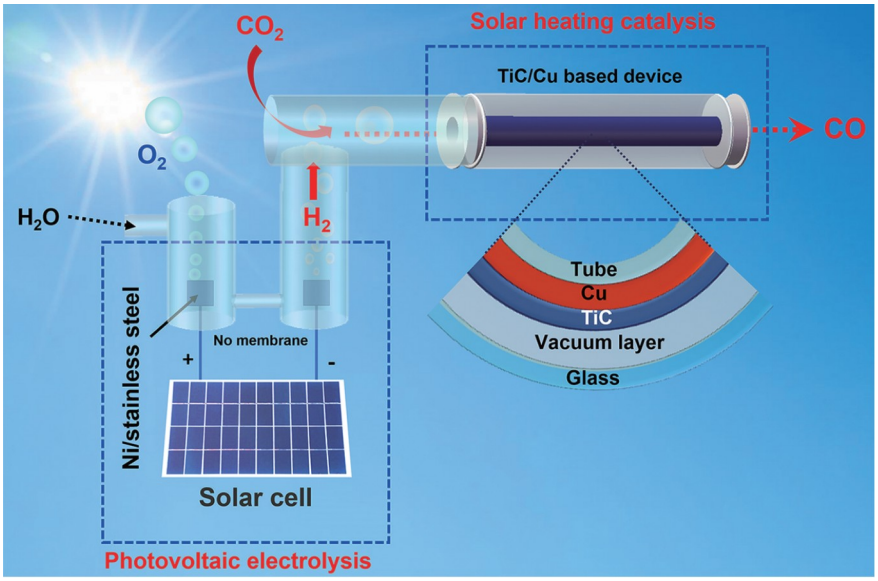

Figure 1 Schematic map of the novel artificial photosynthesis.

second is the quality matching of hydrogen production and hydrogen consumption in the new system.

Integrating the artificial photosynthetic system

A TiC/Cu heterostructure photothermal material was choose to construct the solar heating catalytic system [41–43], which could heat the catalysts to 318°C under 1 kW m^{-2} intensity of sunlight (1 sun) irradiation to run CO_2 hydrogenation (Figure S1). This is the key for realizing the new artificial photosynthetic system, because the low solar irradiated temperature of conventional photothermal system (~80°C, Figure S2) can not drive photothermal CO_2 hydrogenation under ambient solar irradiation. As the Fe single-atom catalysts (Fe SACs, Figures S3–S7) were used as catalysts for solar heating CO_2 hydrogenation, the system showed a CO generation rate of 21.14 mol m^{-2} h^{-1} under 1 sun irradiation, corresponding to 24.1% of solar to chemical energy efficiency (detailed calculation seen in Supplementary Methods, Figure S8). More interestingly, as the 1% O_2-polluted H_2 was used as feed gas, the efficiency of CO_2 hydrogenation had little change (Figure S8A), evidencing the robustness of solar heating catalytic system.

The low requirement of hydrogen purity for solar heating catalysis enables us to simplify the photovoltaic electrocatalysis. Besides using commercialized single crystalline silicon solar cells (23.5% efficiency) as electric energy supply, the membrane was eliminated from the electrocatalytic reactor (Figure 1) and the cheap nickel-plated stainless-steel mesh (Ni/stainless steel, Figure S9) was used as the electrodes to replace the precious electrocatalysts [18–20]. In the membrane free electrocatalytic reactor, the Ni/stainless steel's electrodes could achieve a current density of 10 mA cm^{-2} in 1 mol L^{-1} KOH electrolyte at only 1.53 V (Figure S10). The H_2 production rate of this photovoltaic electrolytic system was 2.40 mol m^{-2} h^{-1} under 1 sun irradiation (Figure S11), equivalent to 19.04% solar to hydrogen chemical efficiency (detailed calculation seen in Supplementary Methods). It was calculated that the solar cell's electric energy to chemicals energy efficiency (EC) of this photovoltaic electrocatalytic water splitting system was 81% (detailed calculation see METHOD SECTION). The released H_2 contained ~0.8% O_2, which also meets the purity requirement of solar heating CO_2 hydrogenation.

Based on the above experimental results, the photovoltaic electrolytic water splitting device with 2800 cm^2 of solar irradiation area and solar heating CO_2 hydrogenation device with 240 cm^2 of solar irradiation area were integrated as a new type of artificial photosynthetic system with more than 3000 cm^2 of solar irradiation area in the laboratory (Figure 1).

The performance of novel artificial photosynthesis

Figure 2A shows that the laboratory system could produce CO with a rate of 38, 210, and 491 mmol h^{-1} under 0.6, 0.8, and 1 sun irradiation, respectively. Additionally, Figure 2B identifies that this system showed a 100% selectivity for CO_2 converted into CO under different intensities of solar irradiation due to the +3 oxidation state of Fe-SACs (Figure S12) [44]. Figure 2C illustrates that the STC of new artificial photosynthetic system was increased from 11.3%, 17.4% to 19.4% along with the 0.6, 0.8 to 1 sun irradiation (detailed calculation see in METHOD SECTION), which was 2.7 times higher than the best record value of scalable artificial photosynthesis with ~1000 cm^2 of solar irradiation area (7.2%) [14]. The CO_2 reduction performance of this system was continuously tested for 6 days. The CO production rate was stable main-

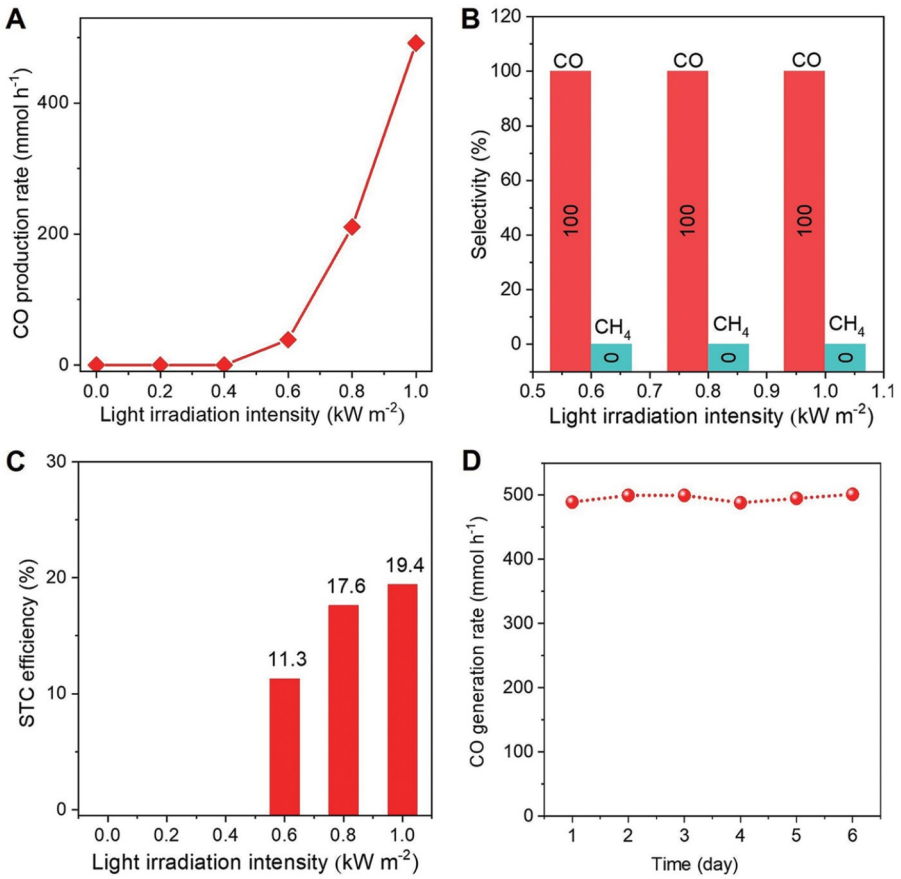

Figure 2 The laboratory performance of novel artificial photosynthetic system. (A) The CO production rate of new artificial photosynthetic system with Fe SACs, under different intensities of solar irradiation. (B) The CO selectivity of new artificial photosynthetic system with Fe SACs, under different intensities of solar irradiation. (C) The STC efficiency of new artificial photosynthetic system with Fe SACs, under different intensities of solar irradiation. (D) The CO production rate stability of new artificial photosynthetic system under 1 sun irradiation.

tained at ~500 mmol h^{-1} (Figure 2D) and the Fe SACs kept single atom state (Figure S13), indicating the excellent stability of new artificial photosynthetic system.

The outdoor artificial photosynthetic demonstration

The commercial single crystalline silicon solar cell panel (1.07 m^2 scale), membrane-free electrolytic water splitting device and factory prepared TiC/Cu based solar heating tube were used to build the outdoor artificial photosynthetic system. For maintaining the solar heating system at high temperature all day, a parabolic reflector with 0.198 m^2 of irradiated area (Figure S14) was applied to concentrate outdoor sunlight on solar heating device (Figure 3A). A commercial $CuO_x/ZnO/Al_2O_3$ (SCST-401, Figure S15) was selected as the catalyst for solar heating reverse water-gas-shift reaction ($CO_2 + H_2 \rightarrow CO + H_2O$). In outdoor test, the membrane-free electrolytic water splitting device was driven by the silicon solar cell panel to produce H_2, and then the H_2 and CO_2 entered the solar heating system for CO_2 hydrogenation (Figure 3B). The artificial photosynthetic system for CO production was tested in December 20, 2021, with an ambient temperature of 2–13°C and a solar irradiation intensity of 0.26–0.49 kW m^{-2} in the daytime in Baoding City of Hebei

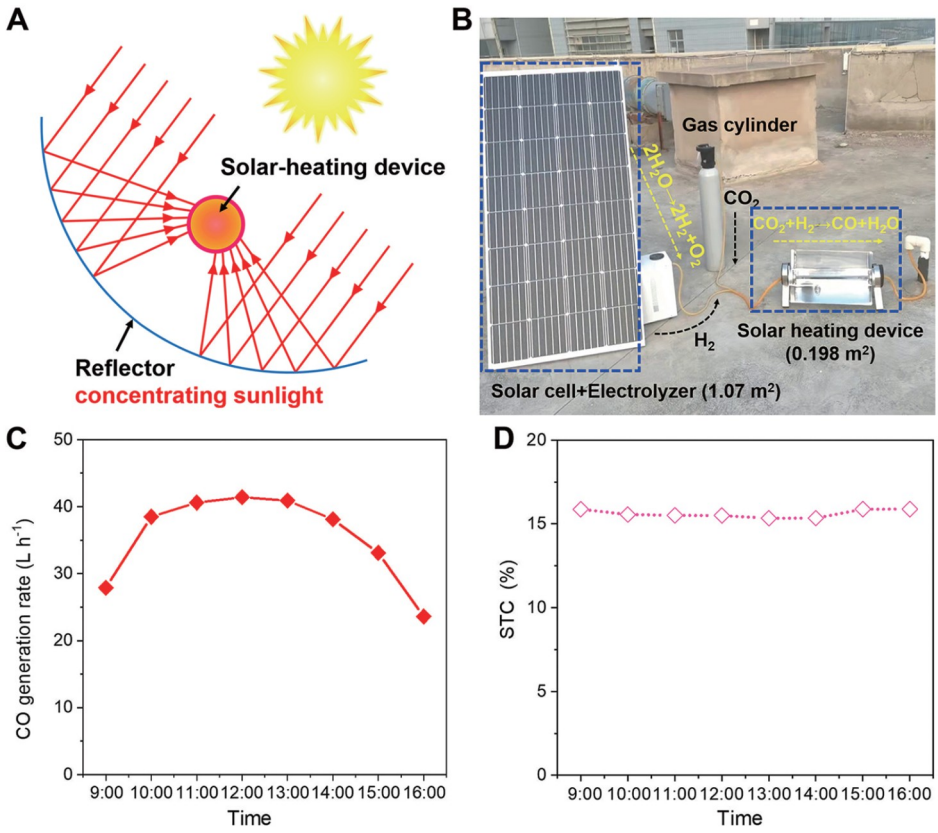

Figure 3 The outdoor performance of novel artificial photosynthetic system. (A) The location diagram of reflector, solar heating device. (B) The photograph of new artificial photosynthetic demonstration on the roof of the building in Hebei University. (C, D) The CO production rate and STC of new artificial photosynthetic demonstration under ambient sunlight irradiation, on December 20, 2021, in Baoding City, China.

Province, China. As shown in Figure 3C, the CO generation occurred at 9:00 AM with a production rate of 27.9 L h^{-1}. After that, the CO generation rate rose to a peak value of 41.4 L h^{-1} at 12:00 PM and then gradually decreased to 23.6 L h^{-1} at 16:00 PM. The total amount of CO produced daily was up to 258.4 L. Although the solar intensity and ambient temperature are the lowest in winter, the outdoor system STC for CO production was still in the range of 15% to 15.8% throughout the operating period (Figure 3D, detailed calculation see METHOD SECTION).

Table 1 lists the data of new artificial photosynthetic systems and the most advanced large-sized artificial photosynthetic systems. Firstly, the size of the outdoor artificial photosynthetic system was 1.268 m^2, and all parts can be processed in the factory, showing that the system could realize mass production directly. Secondly, the STCs of lab and outdoor systems for CO_2 reduction as CO were 19.4% and 15%–15.8% respectively, which were 2.7 times and 4 times higher than that of reported large-sized artificial photosynthetic systems under lab and outdoor conditions, respectively [13,14]. The total cost of outdoor demonstration was calculated as $1018 per m^2 (Figure S16). Table 1 shows that the cost of large-sized artificial photosynthetic devices is too expensive to calculated cost [13,14,45]. Compared with systems that produce mixture of CO and H_2 [13,46], the main product of our artificial photosynthetic system is CO. As far as we known, the cheapest cost of small-sized artificial photosynthetic device reported in literatures was ~$7200

Table 1 Comparison of the solar driven CO_2 reduction systems of this work and the state of the art of solar cells driven artificial photosynthetic systems. IA is the working solar illumination area of device used for CO_2 conversion.

Ref.	Condition	IA (cm^2)	Main product	STC (%)	Cost ($ per m^2)
This work	Outdoor	12,680	CO	15–15.8	1018
[13]	Outdoor	65,000	CO+H_2	3.8	None
[45]	Outdoor	14,700	Formic acid	1.86	None
This work	Lab	2287	CO	19.4	None
[17]	Lab	14	CO	8.05	7200
[14]	Lab	987	Formic acid	7.2	None
[46]	Lab	16	CO+H_2	4.3	None

per m^2 (Table 1) [17], which was 7 times higher than that in our outdoor demonstration. With the ultra-high STC and ultra-low system cost, the system cost recovery time of the outdoor artificial photosynthetic device was calculated by selling product (CO). Referring to the price of CO ($6 per m^3) [17], the outdoor system could recover the cost after 833 days of operation, which corresponds to ~3.5 years (detailed calculation see in METHOD SECTION). The service life of the components in this outdoor system for CO production was generally more than 10 years, able to profitable by selling CO.

CONCLUSIONS

In this work, a novel artificial photosynthesis paradigm was proposed, in which the silicon solar cells were used to drive the membrane free electrolyzer for photovoltaic electrolytic water splitting as O_2 and H_2. Then, the generated H_2 and CO_2 were injected into the solar heating system based on a TiC/Cu based device to carry out efficient sunlight driven CO_2 hydrogenation due to the high 1 sun-heating temperature of 318°C. The photovoltaic electrolytic reactor eliminated the membrane and used the Ni-plated stainless steel mesh as the electrodes to reduce the cost. As the 240 cm^2 of solar heating CO_2 hydrogenation device was integrated to 2800 cm^2 of silicon solar cell driven photovoltaic electrolytic water splitting device, the system exhibited a CO_2 conversion rate of 491 mmol h^{-1}, an STC of 19.4%, a selectivity of 100% for CO production, under 1 sun irradiation. Moreover, an outdoor demonstration with 1.268 m^2 of solar irradiation area was constructed, which showed a cost of $1018 per m^2, the gas production of 258.4 L per day, the STC of 15%–15.8% for CO production in winter, under ambient solar irradiation, which could neutralize device cost by selling the product of CO within 833 sunny operation days, revealing the ability for direct scalable application.

OUTLOOK

The new artificial photosynthetic system has huge space for STC improvement and flexible product regulated ability. As the silicon solar cell was replaced by triple-junction solar cells for photovoltaic electrocatalytic water splitting, the calculated STC of new artificial photosynthetic system was as high as 28.9% (detailed calculation see Supplementary Methods) , which was higher than the best STC (19.1%) of triple-junction solar cells driven artificial photosynthesis [47]. Further, this system could convert product from CO to CH_4

by changing the solar heating CO_2 hydrogenation catalysts as commercial Ni/Al_2O_3 (Figure S17, detailed calculation see Supplementary Methods). Therefore, our system could be a core investigating platform for scientists all over the world to realize carbon neutralization, via converting CO_2 and H_2O into a variety of chemicals, such as methanol, formic acid even C_{2+} product, by developing different catalysts. We believe this new artificial photosynthetic system will speed up the development and application of artificial photosynthesis.

Data availability

The data that support the findings of this study are available from the corresponding authors upon reasonable requests.

Acknowledgements

We thank the transmission electron microscopy (TEM) technical support provided by the Microanalysis Center, College of Physics Science and Technology, Hebei University. Qingbo Meng appreciates the encouragement and recommendation of Professor Yue Zhang of Beijing University of Science and Technology for our work which was published on arXiv: 2204.04971 on 11 Apr. 2022.

Funding

This work was supported by the Natural Science Foundation of Hebei Province (B2022201090, B2021201074, B2021201034 and F2021203097), Hebei Provincial Department of Science and Technology (216Z4303G), Hebei Education Department (QN2022059), the Interdisciplinary Research Program of Natural Science of Hebei University (521100311 and DXK202109) and the Knowledge Innovation Program of the Chinese Academy of Sciences, Hebei University (050001-521100302025 and 050001-513300201004).

Author contributions

Y.L. and Q.M. conceived the project and contributed to the design of the experiments and analysis of the data. Y.L. contributed to the solar heating system strategy. Q.M. proposed the concept for the novel artificial photosynthetic system. S. W. and L.G. contributed to the analysis of the data and the discussion. X.B. and D.Y. performed the TiC/Cu based device preparation and characterizations. X.B., and F.M. performed the catalyst preparation and characterizations. F.M. and X.S. conducted the scanning electron microscopy (SEM) and TEM examinations. Y.L. and Q.M. wrote the paper. All the authors discussed the results and commented on the manuscript.

Conflict of interest

The authors declare no conflict of interest.

Supplementary information

The supporting information is available online at https://doi.org/10.1360/nso/20230033. The supporting materials are published as submitted, without typesetting or editing. The responsibility for scientific accuracy and content remains entirely with the authors.

References

1 Beck A, Zabilskiy M, Newton MA, *et al.* Following the structure of copper-zinc-alumina across the pressure gap in carbon dioxide hydrogenation. *Nat Catal* 2021; **4**: 488–497.

2 Zhou B, Ou P, Pant N, *et al.* Highly efficient binary copper-iron catalyst for photoelectrochemical carbon dioxide

reduction toward methane. *Proc Natl Acad Sci USA* 2020; **117**: 1330–1338.

3 Zhong M, Tran K, Min Y, *et al.* Accelerated discovery of CO_2 electrocatalysts using active machine learning. *Nature* 2020; **581**: 178–183.

4 Wang Y, Liu J, Wang Y, *et al.* Efficient solar-driven electrocatalytic CO_2 reduction in a redox-medium-assisted system. *Nat Commun* 2018; **9**: 5003.

5 Asadi M, Kim K, Liu C, *et al.* Nanostructured transition metal dichalcogenide electrocatalysts for CO_2 reduction in ionic liquid. *Science* 2016; **353**: 467–470.

6 Schreier M, Héroguel F, Steier L, *et al.* Solar conversion of CO_2 to CO using Earth-abundant electrocatalysts prepared by atomic layer modification of CuO. *Nat Energy* 2017; **2**: 17087.

7 Cestellos-Blanco S, Zhang H, Kim JM, *et al.* Photosynthetic semiconductor biohybrids for solar-driven biocatalysis. *Nat Catal* 2020; **3**: 245–255.

8 Yuan H, Cheng B, Lei J, *et al.* Promoting photocatalytic CO_2 reduction with a molecular copper purpurin chromophore. *Nat Commun* 2021; **12**: 1835.

9 Jiang Z, Xu X, Ma Y, *et al.* Filling metal-organic framework mesopores with TiO_2 for CO_2 photoreduction. *Nature* 2020; **586**: 549–554.

10 Xu Y, Li X, Gao J, *et al.* A hydrophobic FeMn@Si catalyst increases olefins from syngas by suppressing C_1 by-products. *Science* 2021; **371**: 610–613.

11 Terrer C, Phillips RP, Hungate BA, *et al.* A trade-off between plant and soil carbon storage under elevated CO_2. *Nature* 2021; **591**: 599–603.

12 Steffens L, Pettinato E, Steiner TM, *et al.* High CO_2 levels drive the TCA cycle backwards towards autotrophy. *Nature* 2021; **592**: 784–788.

13 Schäppi R, Rutz D, Dähler F, *et al.* Drop-in fuels from sunlight and air. *Nature* 2021; **601**: 63–68.

14 Kato N, Mizuno S, Shiozawa M, *et al.* A large-sized cell for solar-driven CO_2 conversion with a solar-to-formate conversion efficiency of 7.2%. *Joule* 2021; **5**: 687–705.

15 Mi Y, Qiu Y, Liu Y, *et al.* Cobalt-iron oxide nanosheets for high-efficiency solar-driven CO_2-H_2O coupling electrocatalytic reactions. *Adv Funct Mater* 2020; **30**: 2003438.

16 Wang J, Zardetto V, Datta K, *et al.* 16.8% Monolithic all-perovskite triple-junction solar cells via a universal two-step solution process. *Nat Commun* 2020; **11**: 5254.

17 Chae SY, Lee SY, Han SG, *et al.* A perspective on practical solar to carbon monoxide production devices with economic evaluation. *Sustain Energy Fuels* 2020; **4**: 199–212.

18 Xu Y, Li F, Xu A, *et al.* Low coordination number copper catalysts for electrochemical CO_2 methanation in a membrane electrode assembly. *Nat Commun* 2021; **12**: 2932.

19 Devasia D, Wilson AJ, Heo J, *et al.* A rich catalog of C–C bonded species formed in CO_2 reduction on a plasmonic photocatalyst. *Nat Commun* 2021; **12**: 2612.

20 Tang C, Gong P, Xiao T, *et al.* Direct electrosynthesis of 52% concentrated CO on silver's twin boundary. *Nat Commun* 2021; **12**: 2139.

21 Li F, Thevenon A, Rosas-Hernández A, *et al.* Molecular tuning of CO_2-to-ethylene conversion. *Nature* 2020; **577**: 509–513.

22 Nam DH, De Luna P, Rosas-Hernández A, *et al.* Molecular enhancement of heterogeneous CO_2 reduction. *Nat Mater* 2020; **19**: 266–276.

23 Ma W, Xie S, Liu T, *et al.* Electrocatalytic reduction of CO_2 to ethylene and ethanol through hydrogen-assisted C–C coupling over fluorine-modified copper. *Nat Catal* 2020; **3**: 478–487.

24 Tahir M, Tasleem S, Tahir B. Recent development in band engineering of binary semiconductor materials for solar driven photocatalytic hydrogen production. *Int J Hydrogen Energy* 2020; **45**: 15985–16038.

25 Qiu XF, Zhu HL, Huang JR, *et al.* Highly selective CO_2 electroreduction to C_2H_4 using a metal-organic framework with dual active sites. *J Am Chem Soc* 2021; **143**: 7242–7246.

26 Yan C, Li H, Ye Y, *et al.* Coordinatively unsaturated nickel-nitrogen sites towards selective and high-rate CO_2 electroreduction. *Energy Environ Sci* 2018; **11**: 1204–1210.

27 Yang HB, Hung SF, Liu S, *et al.* Atomically dispersed Ni(I) as the active site for electrochemical CO_2 reduction. *Nat Energy* 2018; **3**: 140–147.

28 Lee WH, Lim C, Ban E, *et al.* W@Ag dendrites as efficient and durable electrocatalyst for solar-to-CO conversion using scalable photovoltaic-electrochemical system. *Appl Catal B-Environ* 2021; **297**: 120427.

29 Xu Y, Zhang W, Li Y, *et al.* A general bimetal-ion adsorption strategy to prepare nickel single atom catalysts anchored on graphene for efficient oxygen evolution reaction. *J Energy Chem* 2020; **43**: 52–57.

30 Ju T, Zhou YQ, Cao KG, *et al.* Dicarboxylation of alkenes, allenes and (hetero)arenes with CO_2 via visible-light photoredox catalysis. *Nat Catal* 2021; **4**: 304–311.

31 Gu J, Hsu CS, Bai L, *et al.* Atomically dispersed Fe^{3+} sites catalyze efficient CO_2 electroreduction to CO. *Science* 2019; **364**: 1091–1094.

32 Salvatore DA, Gabardo CM, Reyes A, *et al.* Designing anion exchange membranes for CO_2 electrolysers. *Nat Energy* 2021; **6**: 339–348.

33 Jia J, Seitz LC, Benck JD, *et al.* Solar water splitting by photovoltaic-electrolysis with a solar-to-hydrogen efficiency over 30%. *Nat Commun* 2016; **7**: 13237.

34 Li Y, Hao J, Song H, *et al.* Selective light absorber-assisted single nickel atom catalysts for ambient sunlight-driven CO_2 methanation. *Nat Commun* 2019; **10**: 2359.

35 Wang L, Dong Y, Yan T, *et al.* Black indium oxide a photothermal CO_2 hydrogenation catalyst. *Nat Commun* 2020; **11**: 2432.

36 Chen Y, Zhang Y, Fan G, *et al.* Cooperative catalysis coupling photo-/photothermal effect to drive Sabatier reaction with unprecedented conversion and selectivity. *Joule* 2021; **5**: 3235–3251.

37 Rohling JH, Shen J, Wang C, *et al.* Determination of binary diffusion coefficients of gases using photothermal deflection technique. *Appl Phys B* 2007; **87**: 355–362.

38 Belgodere C, Dubessy J, Vautrin D, *et al.* Experimental determination of CO_2 diffusion coefficient in aqueous solutions under pressure at room temperature via Raman spectroscopy: Impact of salinity (NaCl). *J Raman Spectrosc* 2015; **46**: 1025–1032.

39 Jiang X, Nie X, Guo X, *et al.* Recent advances in carbon dioxide hydrogenation to methanol via heterogeneous catalysis. *Chem Rev* 2020; **120**: 7984–8034.

40 Das S, Pérez-Ramírez J, Gong J, *et al.* Core-shell structured catalysts for thermocatalytic, photocatalytic, and electrocatalytic conversion of CO_2. *Chem Soc Rev* 2020; **49**: 2937–3004.

41 Li Y, Bai X, Yuan D, *et al.* General heterostructure strategy of photothermal materials for scalable solar-heating hydrogen production without the consumption of artificial energy. *Nat Commun* 2022; **13**: 776.

42 Li Y, Bai X, Yuan D, *et al.* Cu-based high-entropy two-dimensional oxide as stable and active photothermal catalyst. *Nat Commun* 2023; **14**: 3171.

43 Li Y, Guan Q, Huang G, *et al.* Low temperature thermal and solar heating carbon-free hydrogen production from ammonia using nickel single atom catalysts. *Adv Energy Mater* 2022; **12**: 2202459.

44 Lourenço AC, Reis-Machado AS, Fortunato E, *et al.* Sunlight-driven CO_2-to-fuel conversion: Exploring thermal and electrical coupling between photovoltaic and electrochemical systems for optimum solar-methane production. *Mater Today Energy* 2020; **17**: 100425.

45 White JL, Herb JT, Kaczur JJ, *et al.* Photons to formate: Efficient electrochemical solar energy conversion via reduction of carbon dioxide. *J CO_2 Util* 2014; **7**: 1–5.

46 Urbain F, Tang P, Carretero NM, *et al.* A prototype reactor for highly selective solar-driven CO_2 reduction to synthesis gas using nanosized earth-abundant catalysts and silicon photovoltaics. *Energy Environ Sci* 2017; **10**: 2256–2266.

47 Cheng WH, Richter MH, Sullivan I, *et al.* CO_2 reduction to CO with 19% efficiency in a solar-driven gas diffusion electrode flow cell under outdoor solar illumination. *ACS Energy Lett* 2020; **5**: 470–476.